Solitons under spatially localized cubic-quintic-septimal nonlinearities

H Fabrelli[1], **J B Sudharsan**[2], **R Radha**[2], **A Gammal**[1] **and Boris A Malomed**[3,4]

[1] Instituto de Física, Universidade de São Paulo, 05508-090, São Paulo, Brazil
[2] Center for Nonlinear Science (CeNSc), PG and Research Department of Physics, Government College for Women (Autonomous), Kumbakonam 612001, Tamil Nadu, India
[3] Department of Physical Electronics, School of Electrical Engineering, Tel Aviv University, Tel Aviv 69978, Israel
[4] Laboratory of Nonlinear-Optical Informatics, ITMO University, St. Petersburg 197101, Russia

E-mail: vittal.cnls@gmail.com

Abstract
We explore stability regions for solitons in the nonlinear Schrödinger equation with a spatially confined region carrying a combination of self-focusing cubic and septimal terms, with a quintic one of either focusing or defocusing sign. This setting can be implemented in optical waveguides based on colloids of nanoparticles. The solitons' stability is identified by solving linearized equations for small perturbations, and is found to fully comply with the Vakhitov–Kolokolov criterion. In the limit case of tight confinement of the nonlinearity, results are obtained in an analytical form, approximating the confinement profile by a delta-function. It is found that the confinement greatly increases the largest total power of stable solitons, in the case when the quintic term is defocusing, which suggests a possibility to create tightly confined high-power light beams guided by the spatial modulation of the local nonlinearity strength.

Keywords: nonlinear Schrodinger equation, collisional inhomogeneity, cubic-quintic-septimal, solitons

(Some figures may appear in colour only in the online journal)

1. Introduction

The importance of spatial solitons, which are maintained by the balance between diffraction and self-focusing, in modern photonics is commonly known [1–8]. In particular, the ubiquitous Kerr self-focusing nonlinearity is modeled by the cubic nonlinear Schrödinger equation (NLSE), which predicts stable solitons in optical fibers and planar waveguides, as well as in many other systems [2]. On the other hand, more complex effects, such as the generation of higher-order harmonics [9], filamentation [10], saturation of the Kerr nonlinearity [11], modulational instability in metamaterials [12], creation of quasi-stable optical beams with embedded vorticity [13], and other nonlinear phenomena make it necessary to add higher-order nonlinearities to the NLSE. In particular, the recently reported stable propagation of (2+1)-dimensional

fundamental spatial solitons in bulk dielectric media is explained by the action of the cubic-quintic (CQ) [14] or quintic-septimal [15] nonlinearities, in which the sign of the higher term is defocusing. It was also predicted that the CQ nonlinearity is sufficient to support stable two- [16] and three-[17] dimensional (2D and 3D) solitons with embedded vorticity.

Recently, it has been demonstrated that various combinations of optical nonlinearities, including CQ and septimal terms of either sign, can be engineered in colloids composed of metallic nanoparticles [18]. This finding has suggested a detailed analysis of 1D solitons under the action of the combined cubic-quintic-septimal (CQS) nonlinearity [19], the most essential issue being stability of such soliton families for different combinations of signs in front of the CQS terms. In particular, a noteworthy result is that, in spite of the well-known fact that the

focusing quintic and septimal terms give rise, respectively, to the critical and supercritical collapse in the 1D NLSE [20, 21], the 1D equation with the focusing signs of all the nonlinear terms in the CQS combination maintains stable soliton families (similar to the previously known fact that the combination of self-attractive cubic and quintic terms also generates stable solitons [22]).

Another direction of the work with nonlinearity, which has also drawn much attention in the course of the last decade, is the use of spatially modulated nonlinear terms for the creation and stabilization of various species of solitons [5]. In particular, a stepwise radial change of the local strength of the cubic self-focusing is sufficient to stabilize Townes solitons in the 2D space [23]. It has also been recently observed that the spatially modulated nonlinearity can contribute to an earlier onset of Faraday and resonant waves [7, 8]. It was also demonstrated that stable 2D solitons with embedded higher-order vorticity, up to $S = 6$, can be supported by localized cubic self-focusing in a combination with the harmonic-oscillator trapping potential [24], while previously no stable states with $S \geqslant 2$ could be constructed using local nonlinearity and trapping potentials [3, 5].

The above-mentioned findings suggest to seek for possibilities to predict stable solitons supported by the CQS nonlinearity subject to the spatial modulation, which is the objective of the present work. In effectively planar waveguides built of the above-mentioned colloidal materials, which provide the CQS nonlinearity for the creation of spatial solitons, the modulation can be induced by making the waveguide's thickness a function of the propagation distance. Higher-order nonlinearities may also be provided by resonant dopants (see, e.g., [25]), in which case the spatial modulation is naturally imposed by inhomogeneity of the dopant density along the propagation distance. We focus on the most interesting 'sandwich' setting, when the lowest and highest cubic and septimal terms are self-focusing, while the intermediate quintic one may have either sign. A challenge is to secure stability of the solitons when, in particular, the competition between focusing and defocusing (quintic) terms may support stable solitons, in spite of the possibility of the onset of the supercritical collapse, driven by the septimal self-focusing term. The model, based on an appropriate version of the NLSE, is introduced in section 2. Accurate results of a systematic numerical analysis, focused on the solitons' stability, are reported in section 3. For the limiting case of tight confinement of the nonlinearity, approximate analytical results, which are found to be in good agreement with the numerical counterparts, and thus help to explain the numerical findings, are presented in section 4. The paper is concluded in section 5.

2. The model

The 1D NLSE for amplitude $\Psi(x, z)$ of the electromagnetic wave with spatially-localized CQS nonlinear terms is written

in the scaled form for the spatial domain as

$$i\frac{\partial \Psi}{\partial z} + \frac{1}{2}\frac{\partial^2 \Psi}{\partial x^2} + [G_3(x)P|\Psi|^2 + G_5(x)P^2|\Psi|^4 + G_7(x)P^3|\Psi|^6]\Psi = 0, \tag{1}$$

with normalization condition

$$\int_{-\infty}^{+\infty} |\Psi(x, z)|^2 \mathrm{d}x = 1 \tag{2}$$

and total power P. Here z and x are the propagation distance and transverse coordinate, and x-dependent coefficients in front of the cubic, quintic, and septimal ($n = 3, 5, 7$, respectively) terms are defined as

$$G_n(x) = g_n \exp(-b^2 x^2/2), \tag{3}$$

where b determines the size of the nonlinearity-bearing region, $|x| \lesssim 1/b$. Further, being interested, as said above, in the case when both the cubic and septimal terms are self-focusing, we use the possibility to rescale the variables and parameters in equations (1) and (3), as

$$z \equiv \sqrt{g_7/g_3^3}\, z', \quad x \equiv (g_7/g_3^3)^{1/4}x',$$
$$\Psi \equiv (g_3^3/g_7)^{1/8}\Psi',$$
$$P \equiv (g_3 g_7)^{-1/4}P', \quad b \equiv (g_3^3/g_7)^{1/4}b', \tag{4}$$

so as to fix the accordingly transformed cubic and septimal coefficients (primes appearing in equation (4) are dropped below),

$$g_3 = g_7 = 1, \tag{5}$$

while b, g_5 and P are kept as irreducible control parameters, $g_5 > 0$ and < 0 corresponding, severally, to the focusing and defocusing quintic terms. Of course, the normalization conditions (5) may be chosen in a different from, if that may be more convenient for some purposes.

The dynamical model based on equation (1) with $g_5 > 0$ can be also derived as an approximate form of the Gross–Pitaevskii equation (GPE) for a relatively dense atomic Bose–Einstein condensate with attractive inter-atomic interactions. Starting from the 3D GPE with the cubic self-attractive nonlinearity, the reduction of the dimension from 3D to 1D for a condensate tightly trapped in a cigar-shaped potential leads to the NLSE for the 1D mean-field wave function $\Psi(x, t)$ with non-polynomial nonlinearity $\sim[1 - (3/2)g|\Psi|^2](1 - g|\Psi|^2)^{-1/2}\Psi$, where $g > 0$ is an effective self-attraction coefficient [26]. The truncated expansion of this expression in powers of $|\Psi|^2$ up to the third order leads to the NLSE in the form of equation (1), with $G_5 \sim g^2 > 0$, and z replaced by scaled time t. The spatial modulation of the nonlinearity coefficient, $g(x)$, can be imposed by means of the experimentally available method based on the Feshbach resonance controlled by a spatially inhomogeneous optical [27] or magnetic [24] field.

Stationary states with propagation constant k are looked for as solutions to equation (1) in the form of $\Psi(x, z) = \psi(x)e^{ikz}$, with real function $\psi(x)$ satisfying the ordinary

differential equation,

$$k\psi = \frac{1}{2}\frac{d^2\psi}{dx^2} + \exp\left(-\frac{1}{2}b^2x^2\right)P\psi^3(1 + g_5P\psi^2 + P^2\psi^4).$$
(6)

Stability of the stationary states is addressed by taking perturbed solutions as $\Psi(x, t) = [\psi(x) + \delta\psi(x, z)]\exp(ikz)$, where small perturbation $\delta\psi(x, t)$ evolves according to the linearized equation,

$$\left(i\frac{\partial}{\partial z} - k + \frac{1}{2}\frac{\partial^2}{\partial x^2}\right)\delta\psi + \exp\left(-\frac{1}{2}b^2x^2\right)P\psi^2(x)$$
$$\times [(\delta\psi^* + 2\delta\psi) + g_5P\psi^2(x)(2\delta\psi^* + 3\delta\psi)$$
$$+ P^2\psi^4(x)(3\delta\psi^* + 4\delta\psi)] = 0,$$
(7)

with * standing for the complex conjugate. For perturbation eigenfunctions sought for in the usual form [28–31], $\delta\psi(x, z) = u(x)\exp(i\lambda z) + v^*(x)\exp(-i\lambda^*z)$, the corresponding eigenvalue problem for λ amounts to the system of coupled linear equations:

$$\frac{1}{2}\frac{d^2u}{dx^2} + \exp\left(-\frac{1}{2}b^2x^2\right)P\psi^2(x)[(2u + v)$$
$$+ g_5P\psi^2(x)(3u + 2v) + P^2\psi^4(x)(4u + 3v)]$$
$$- ku = \lambda u,$$
$$\frac{1}{2}\frac{d^2v}{dx^2} + \exp\left(-\frac{1}{2}b^2x^2\right)P\psi^2(x)[(2v + u)$$
$$+ g_5P\psi^2(x)(3v + 2u) + P^2\psi^4(x)(4v + 3u)]$$
$$- kv = -\lambda v.$$
(8)

As usual, the stability condition is that all eigenvalues λ (eigenfrequencies of the small-perturbation modes) must be purely real.

Stationary equation (6) was solved numerically by means of a relaxation algorithm, which is outlined in [32], starting with spatial stepsize $\Delta x = 0.01$, and reducing it for solutions with a shrinking size. For the verification of the results, stationary solutions were also produced, for $g_5 > 0$ and $b > 2$, with the help of a shooting Runge–Kutta algorithm, as described in [33]. The time evolution governed by equation (1) was simulated using a Crank–Nicolson algorithm [34], with spatial stepsizes similar to the above-mentioned ones, employed for the realization of the relaxation method, and temporal step $\Delta t = 0.001$.

The linear system (8) was solved, using $\psi^2(x)$ produced by the relaxation method, and putting the system on a spatial grid composed of up to 1000 points. For carrying out the solution procedure, the corresponding matrix was diagonalized using a LAPACK routine [35], which eventually provided all the eigenvalues.

3. Numerical results

Typical examples of numerically found solitons, along with their counterparts predicted by the analytical approximation (see equations (13) and (15) below), are displayed in figure 1. The shape of the solitons supported by the confined nonlinearity is close to that of *peakons*, which are usually produced by models with nonlinear dispersion, such as the Camassa–Holm equation [36] and the continual limit of the Salerno model [37] with competing on-site and inter-site cubic terms [38].

Further, in figure 2 we present characteristics of numerically found stationary soliton families, provided by the dependence of the propagation constant, k, on the total power, P, as obtained from the numerical solution of equation (6) for $g_5 = -1$ and $g_5 = +1$, i.e., defocusing and focusing signs of the quintic term, with different values of parameter b which determines the inverse width of the nonlinearity-localization region in equation (3). The stability of the soliton families is also shown in figure 2.

At $g_5 < 0$ (the defocusing sign of the quintic term) and each b, the stable solitons exist in the interval of $P_{min}(g_5 < 0; b) < P < P_{max}(g_5 < 0; b)$, with $P_{min}(g_5 < 0; b)$ and $P_{max}(g_5 < 0; b)$ given (in an approximate form) by equation (18) presented below. These smallest and largest values of the total power are designated by bold dots in figure 2.

In the limit of $k \to \infty$, the soliton solution, subject to normalization condition (2), becomes very narrow (hence it does not depend on the value of b), with the shape dominated by the septimal term:

$$\psi_{k\to\infty}(x) \approx \frac{k^{1/4}}{[\cosh(3\sqrt{2k}\,x)]^{1/3}},$$
(9)

where the limit form of the $k(P)$ relation is

$$k \approx 15.2 \cdot P^{-6}$$
(10)

(numerical factors in equations (9), in which the factor is very close to 1, and (10) are determined by the value of coefficient $\int_{-\infty}^{+\infty}(\operatorname{sech} x)^{2/3}\,dx \approx 4.2$). The range of (very large) values of k in which the asymptotic solution, given by equations (9) and (10), is valid, is not shown in figure 2 because the solutions are completely unstable in that case, as equation (10) does not meet the Vakhitov–Kolokolov (VK) criterion, which is discussed in detail below (the instability is also corroborated by numerical results).

It is worth noting that the self-defocusing sign of the quintic term, $g_5 < 0$, provides for the expansion of the existence and stability limit to much greater values of the total power, P. While this result is quite natural in the case of the CQS nonlinearity, it is relevant to stress that a formally similar combination of the focusing quintic and defocusing cubic nonlinearities, in the absence of the septimal term, gives rise to completely unstable solitons [22]. In the present case, the stabilization is provided by the presence of the focusing term with the lowest (cubic) nonlinearity, which is absent in the above-mentioned CQ setting. As for the situation with the focusing quintic term, $g_5 > 0$, which is displayed in figure 2(b), it is relevant to stress that each $k(P)$ curve features a stability segment.

Furthermore, it is noteworthy too that, taking larger b, i.e., a narrower nonlinearity-localization region in equation (3), which is the most essential feature of the present model, also helps to
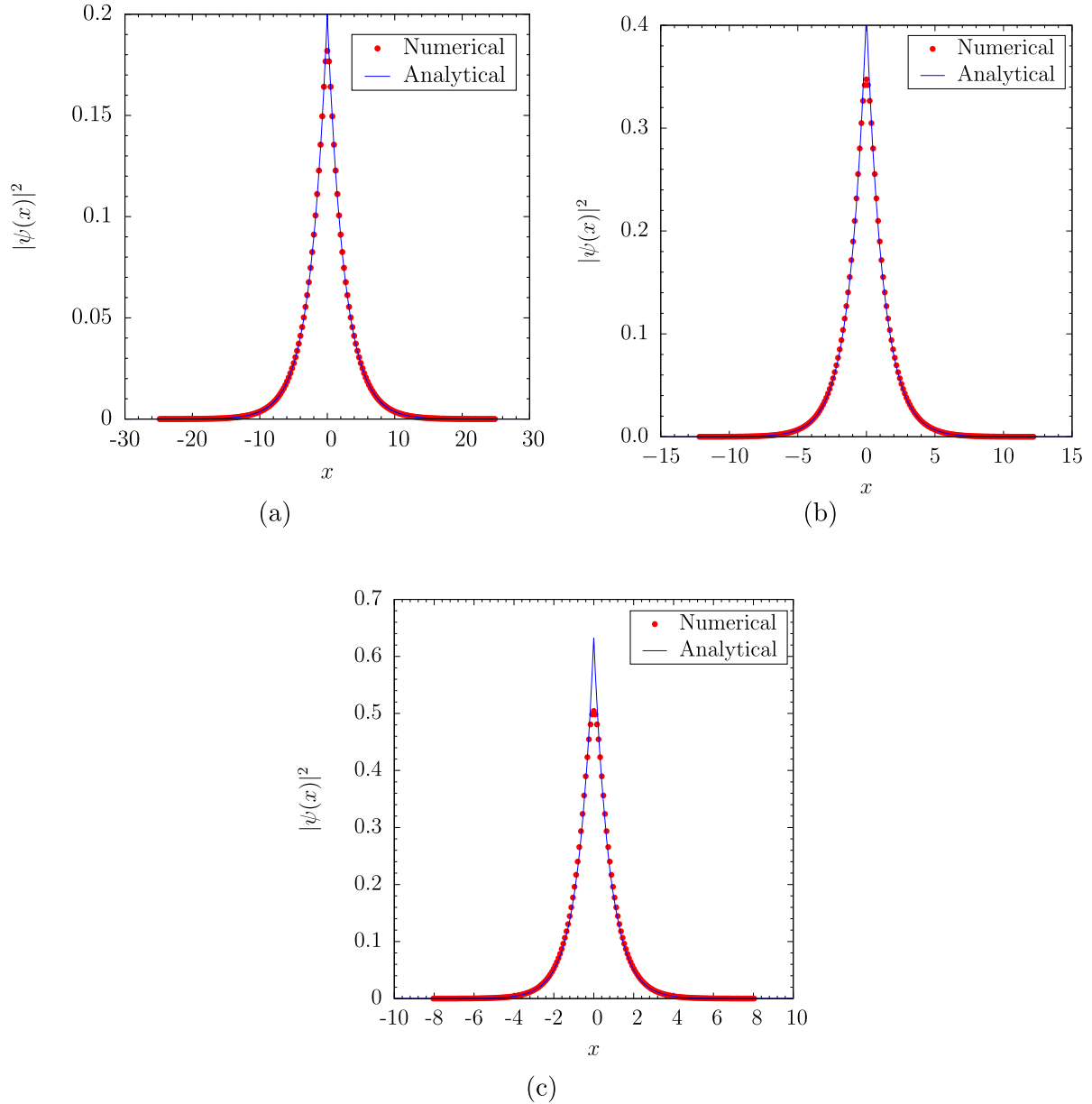
Figure 1. Chains of dots show solitons produced by the numerical solution of equation (6) with $b = 3$ and $g_5 = -1$, along with solutions predicted by the analytical approximation based on equations (13) and (15). The propagation constants of the solutions are (a) $k = 0.02$, $P = 1.89$ (a stable solution), (b) $k = 0.085$, $P = P_{max} = 2.22$ (at the stability boundary, see figure 2 below), and (c) $k = 0.2$, $P = 2.13$ (an unstable solution).

extend the stability region of P. This effect is quite conspicuous, in figure 2(a), for $g_5 < 0$, while for $g_5 > 0$ the stability interval expands, in figure 2(b), up to some critical value of b, which is followed by the transition to completely unstable soliton families. These observations suggests to consider the limit form of the model with the modulation represented by the delta-function, instead of the Gaussian in equation (3), which admits an exact analytical solution, as shown in the next section.

In the typical $k(P)$ plots displayed in figure 2, each curve has a single boundary between unstable and stable (if any)

segments. In a more special case, occurring at $g_5 > 0$ (the fully focusing nonlinearity) near the transition between partly stable and fully unstable soliton families, $k(P)$ curves feature stable segments located between two unstable ones, i.e., in a narrow interval of $P_{min} < P < P_{max}$, as can be seen in figure 3. In particular, the stability regions displayed in the figure resemble results reported in [39] for a liquid–gas phase transition.

The largest total power, P_{max}, up to which stable solitons exist, is an obviously important characteristic of the model
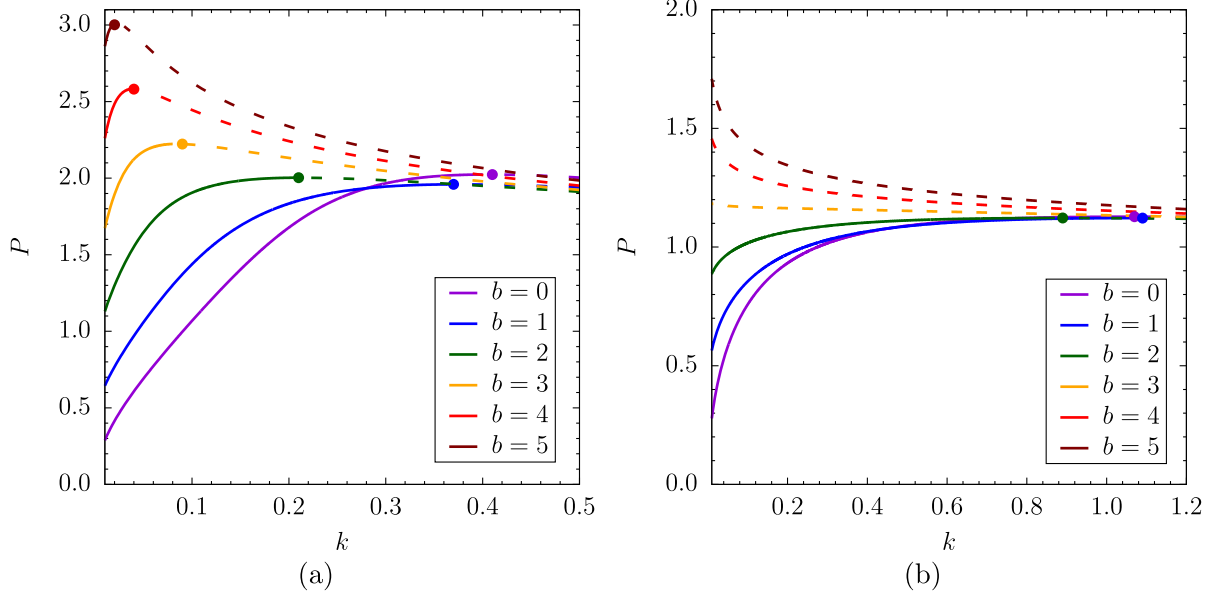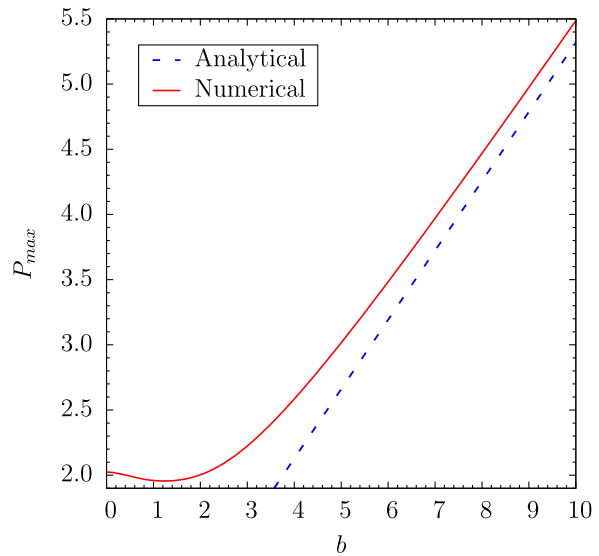
Figure 2. Propagation constant k, as a function of total power P, for soliton families produced by the numerical solution of equation (6) with (a) $g_5 = -1$ and (b) $g_5 = +1$, which correspond, respectively, to the self-defocusing and focusing quintic term, at different values of the inverse-width parameter, b in equation (3) ($b = 0$ corresponds to the spatially uniform nonlinearity). Solid and dashed segments represent, severally, to stable and unstable solutions, according to eigenvalues produced by the numerical solution of equation (8) (the VK criterion predicts exactly the same stability regions, see the text). Bold dots designate the largest and smallest values of the power, P_{max} and P_{min}, see equations (18) and (16) below. In (a), all stable branches originate, at $k = 0$, from points $P = P_{min}(g_5 < 0; b)$, and in (b) the unstable branches (those corresponding to $b = 3, 4, 5$) terminate at points with $k = 0$ and $P = P_{max}(g_5 > 0; b)$.
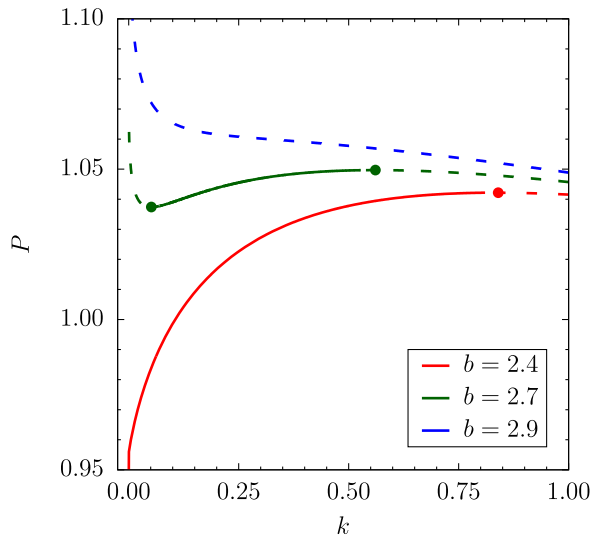
Figure 3. The same as in figure 2, but for $g_5 = 1.5$ (the self-focusing quintic term), in a narrow interval of values of b around the point of the transition from partly stable soliton families to completely unstable ones.
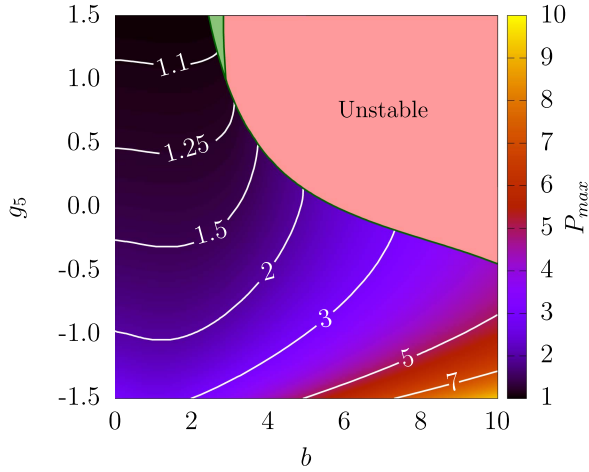
Figure 4. The largest total power P_{max} for families of stable solitons in figure 2(a) as a function of b, for $g_5 = -1$. The red curve summarizes numerical results, while the blue one represents the analytical result produced by the delta-functional limit, see equation (18).

with finite b and $g_5 < 0$, as suggested by figure 2(a). This dependence is displayed in figure 4, along with the analytical prediction obtained in the delta-functional limit.

　　Results of the systematic numerical analysis are summarized in figure 5, which displays P_{max} as a function of both

control parameters, g_5 and b, in a broad area, $(0 \leqslant b \leqslant 10) \times (-1.5 \leqslant g_5 \leqslant +1.5)$. This map shows, in the general form, the trend which was stressed above in the connection to figures 2 and 4, *viz.*, that, at $g_5 \leqslant 0$, the increase

Figure 5. The map of the largest total power of stable solitons, P_{max}, in the (b, g_5) parameter plane, as obtained from the solutions of equations (1)–(5). P_{max} keeps a constant value along each white curve. In the narrow green wedge, stable soliton families feature essentially the same structure as demonstrated by the curve for $b = 2.7$ in figure 3.

Figure 6. Top views of the simulated evolution of solutions for $g_5 = 1.5$ and $b = 2.7$, with $k = 0.04$, $P = 1.038$ (a); $k = 0.25$, $P = 1.045$ (b); and $k = 0.7$, $P = 1.049$ (c).

of b, i.e., narrowing of the spatial localization of the non-linearity, leads to strong increase of the largest total power of the stable solitons. This effect may find various applications, such as strong confinement of powerful light beams in a narrow guiding channel by means of the spatial modulation of the local nonlinearity, in the context of the general topic of nonlinear light guiding [5].

In addition to the accurate computation of the eigenvalues based on equation (8), the stability of the soliton families can be determined by dint of the VK criterion [20, 40], which gives the necessary stability condition in the form of $dk/dN > 0$ (in the general case, the VK criterion is not sufficient for the stability, although in relatively simple settings, such as the present ones, it may be sufficient). As is clearly seen in figures 2 and 3, in the present model the VK criterion is, indeed, not only necessary but also sufficient for the stability, as it precisely predicts the stability areas, identified by the condition of Im $\{\lambda\} = 0$ (see equation (8)).

The so predicted stability/instability of the solitons was tested by direct simulations of their propagation, as shown in figures 6 and 7. In particular, at $g_5 = 1.5$, $b = 2.7$, and $k = 0.04$, $P = 1.038$, the soliton with broad tails (their size may be estimated as $\sim k^{-1/2}$, see equation (9)), which, according to figure 3, is unstable, spontaneously transforms into a robust breather with a small amplitude of internal vibrations, as shown in figures 6(a) and 7(a). On the other hand, figures 6(c) and 7(c) demonstrate that an unstable soliton with essentially shorter tails, corresponding to $k = 0.7$, $P = 1.049$, suffers the collapse. Lastly, the predicted stability of a typical soliton with $k = 0.25$, $P = 1.045$ is confirmed by the simulations displayed in figures 6(b) and 7(b).
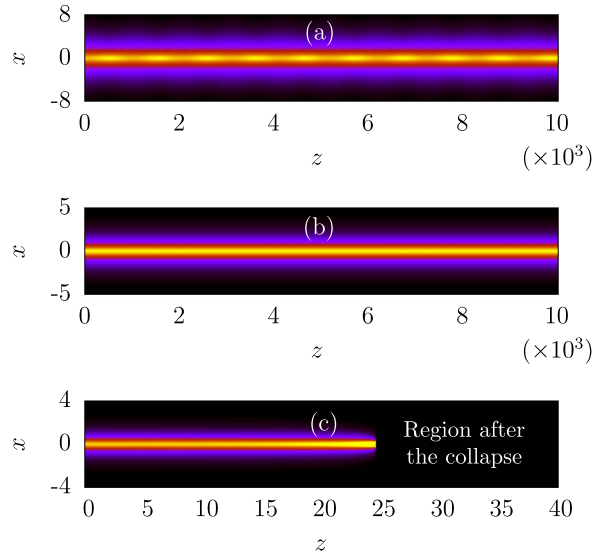
4. The analytical solution in the limit of the delta-functional modulation profile

As mentioned above, the model produces noteworthy results, such as the possibility to support the transmission of tightly confined high-power beams, at large values of b. In this case, the narrow Gaussian in equation (3) may be approximated by the delta-function:

$$\exp(-b^2 x^2/2) \approx \sqrt{2\pi} b^{-1} \delta(x). \tag{11}$$

Then, equation (6) is replaced by

$$k\psi = \frac{1}{2}\frac{d^2\psi}{dx^2} + \frac{\sqrt{2\pi}}{b}\delta(x)P\psi^3(1 + g_5 P\psi^2 + P^2\psi^4). \tag{12}$$

At $x \neq 0$, equation (12) amounts to a linear equation, $\psi'' = -2\mu\psi$, whose solution, satisfying normalization condition (2), is
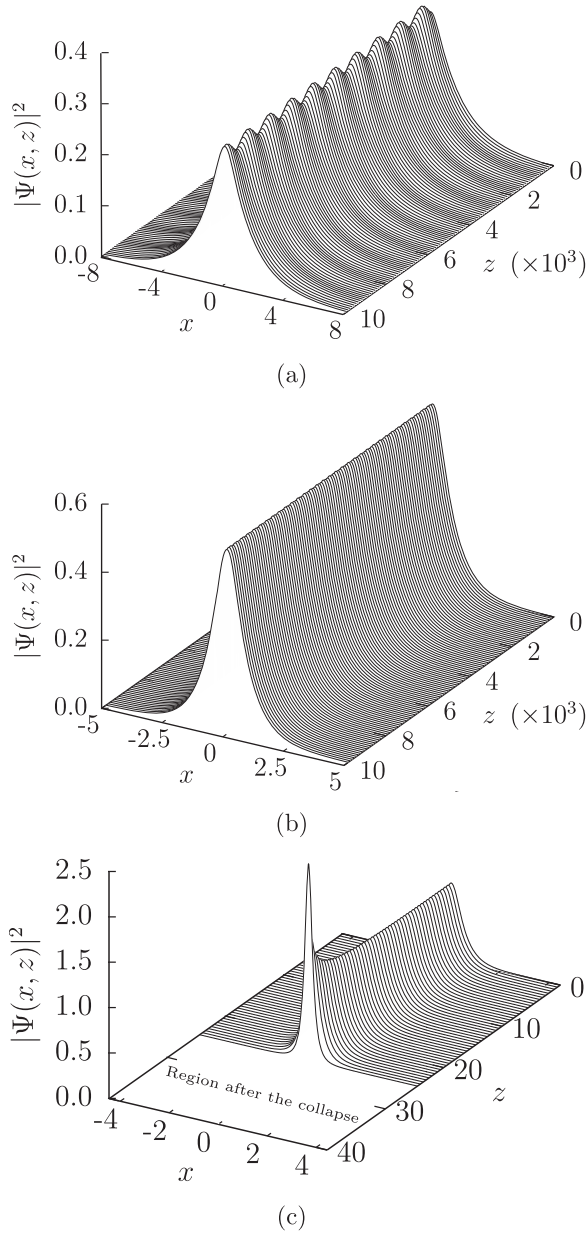
$$\psi(x) = (2k)^{1/4}\exp(-\sqrt{2k}|x|). \tag{13}$$

The integration of equation (12) in an infinitesimal vicinity of $x = 0$ gives rise to the following boundary condition at $x = 0$, assuming that $\psi(x)$ is an even function:

$$\frac{d\psi}{dx}\Big|_{x=+0} = -\frac{\sqrt{2\pi}}{b}P\psi^3(1 + g_5 P\psi^2 + P^2\psi^4)\Big|_{x=+0}. \tag{14}$$

The substitution of solution (13) in equation (14) yields a quadratic equation for $\sqrt{k}$, which determines it as a function of P:

$$2P^3 k + g_5 P^2\sqrt{2k} + \left(P - \frac{b}{\sqrt{2\pi}}\right) = 0. \tag{15}$$

Figure 7. The evolution of an unstable soliton for $k = 0.04$, $P = 1.038$ (a), stable soliton for $k = 0.25$, $P = 1.045$ (b), and unstable soliton for $k = 0.7$, $P = 1.049$ (c), which correspond, respectively, to panels (a)–(c) of figure 6.

As said above, an important characteristic of the soliton families is the largest value P_{max} of the total power, up to which the solitons exist. A straightforward analysis of equation (15) yields, for $g_5 > 0$ (i.e., the self-focusing quintic term),

$$P_{max}(g_5 > 0; b) = b/\sqrt{2\pi}. \qquad (16)$$

At $P < P_{max}(g_5 > 0; b)$, there is a single soliton family with $dk/dP < 0$, which is definitely unstable, according to the VK criterion. Note that $P_{max}(g_5 > 0; b)$ given by equation (16) does

not depend on g_5 (as long as g_5 is positive). These analytical findings, including the values of $P_{max}(g_5 > 0; b)$ given by equation (16), are in good agreement with the numerical counterparts displayed in figure 2(b) for $b \geqslant 3$.

Further, the analysis of equation (15) for $g_5 < 0$ demonstrates that it generates two branches of the $k(P)$ dependence. The branch satisfying the VK criterion, $dk/dP > 0$, exists in a finite interval of values of the power, under restriction $|g_5| < 2$:

$$P_{min}(g_5 < 0; b) = \frac{b}{\sqrt{2\pi}} < P < P_{max}(g_5 < 0; b) \qquad (17)$$

$$= \frac{b}{\sqrt{2\pi}}\left(1 - \frac{g_5^2}{4}\right)^{-1}. \qquad (18)$$

Equation (18) correctly explains an asymptotically linear dependence $P_{max}(g_5 = -1; b)$ at large b, which is clearly seen in figure 4. In particular, the slope of the asymptotic dependence is exactly predicted by equation (18). Subsequent consideration of equation (15) readily shows that $P_{max}(g_5 < 0) = \infty$ at $g_5 \leqslant -2$, which actually implies that there remains a single $k(P)$ branch, with $dk/dP < 0$, i.e., a completely unstable one.

5. Conclusion

In this work, we have addressed the question of how the recently demonstrated stability area for solitons supported by the NLSE with the CQS nonlinearity is affected by the spatial confinement of the nonlinearity, which may be realized in optical waveguides based on colloids of nanoparticles. In particular, it was demonstrated that the localization greatly increases the largest power of the stable guided beams, which opens a path to transmit narrow high-power beams by means of the nonlinear confinement. The stability of the spatial solitons in this model is completely determined by the VK criterion. The results were obtained by means of the systematic numerical analysis, and also in the analytical form, valid in the limit of the tight localization of the nonlinearity.

It may be interesting to extend the analysis for a system of two parallel nonlinearly confined waveguides, thus implementing a nonlinear coupler. A challenging possibility is to explore a 2D generalization of the present model that would imply a nonlinear core embedded in a linear bulk medium (see a similar model with the self-focusing cubic-only nonlinearity, considered in [23]).

Acknowledgments

ORCID

Boris A Malomed ⦿ https://orcid.org/0000-0001-5323-1847

References

[1] Buryak A V, Di Trapani P, Skryabin D V and Trillo S 2002 *Phys. Rep.* **370** 63

[2] Kivshar Y S and Agrawal G P 2003 *Optical Solitons: From Fibers to Photonic Crystals* (San Diego, CA: Academic)

[3] Malomed B A, Mihalache D, Wise F and Torner L 2005 *J. Opt. B: Quantum Semiclass. Opt.* **7** R53
Malomed B A, Mihalache D, Wise F and Torner L 2016 *J. Phys. B: At. Mol. Opt. Phys.* **49** 170502

[4] Kartashov Y V, Vysloukh V A and Torner L 2009 *Prog. Opt.* **52** 63

[5] Kartashov Y V, Malomed B A and Torner L 2011 *Rev. Mod. Phys.* **83** 247

[6] Chen Z, Segev M and Christodoulides D N 2012 *Rep. Prog. Phys.* **75** 086401

[7] Balaz A, Paun R, Nicolin A I, Sudharsan J B and Radha R 2014 *Phys. Rev. A.* **89** 023609

[8] Sudharsan J B, Radha R, Raportaru M C, Nicolin A I and Balaz A 2016 *J. Phys. B: At. Mol. Opt. Phys.* **49** 165303

[9] Moll K D, Homoelle D, Gaeta A L and Boyd R W 2002 *Phys. Rev. Lett.* **88** 153901
Weerawarne D L, Gao X, Gaeta A L and Shim B 2015 *Phys. Rev. Lett.* **114** 093901

[10] Béjot P, Kasparian J, Henin S, Loriot V, Vieillard T, Hertz E, Faucher O, Lavorel B and Wolf J-P 2010 *Phys. Rev. Lett.* **104** 103903

[11] Brée C, Demircan A and Steinmeyer G 2011 *Phys. Rev. Lett.* **106** 183902

[12] Saha M and Sarma A K 2013 *Opt. Commun.* **291** 321

[13] Reyna A S, Malomed B A and de Araújo C B 2015 *Phys. Rev. A* **92** 033810

[14] Falcão-Filho E L, de Araújo C B, Boudebs G, Leblond H and Skarka V 2013 *Phys. Rev. Lett.* **110** 013901

[15] Reyna A S, Jorge K C and de Araújo C B 2014 *Phys. Rev. A* **90** 063835

[16] Quiroga-Teixeiro M and Michinel H 1997 *J. Opt. Soc. Am. B* **14** 2004
Pego R L and Warchall H A 2002 *J. Nonlinear Sci.* **12** 347

[17] Mihalache D, Mazilu D, Crasovan L-C, Towers I, Buryak A V, Malomed B A, Torner L, Torres J P and Lederer F 2002 *Phys. Rev. Lett.* **88** 073902

[18] Falcão-Filho E L, de Araújo C B and Rodrigues J J Jr 2007 *J. Opt. Soc. Am. B* **24** 2498
Reyna A S and de Araújo C B 2014 *Phys. Rev. A* **89** 063803
Reyna A S and de Araújo C B 2014 *Opt. Express* **22** 22456

[19] Reyna A S, Malomed B A and de Araújo C B 2015 *Phys. Rev. A* **92** 033810

[20] Bergé L 1998 *Phys. Rep.* **303** 259
Kuznetsov E A and Dias F 2011 *Phys. Rep.* **507** 43

[21] Rasmussen J J and Rypdal K 1986 *Phys. Scr.* **33** 481

[22] Pelinovsky D E, Kivshar Y S and Afanasjev V V 1998 *Physica D* **116** 121

[23] Sakaguchi H and Malomed B A 2012 *Opt. Lett.* **37** 1035

[24] Sudharsan J B, Radha R, Fabrelli H, Gammal A and Malomed B A 2015 *Phys. Rev. A* **92** 053601

[25] Zubairy M S, Matsko A B and Scully M O 2002 *Phys. Rev. A* **65** 043804

[26] Salasnich L 2002 *Laser Phys.* **12** 198
Salasnich L, Parola A and Reatto L 2002 *Phys. Rev. A* **65** 043614

[27] Yamazaki R, Taie S, Sugawa S and Takahashi Y 2010 *Phys. Rev. Lett.* **105** 050405

[28] Yang J 2010 *Nonlinear Waves in Integrable and Nonintegrable Systems* (Philadelphia, PA: SIAM)

[29] Pushkarov K I, Pushkarov D I and Tomov I V 1979 *Opt. Quantum Electron.* **11** 471
Abdullaev F K and Garnier J 2005 *Phys. Rev. E* **72** 035603

[30] Skarka V, Berezhiani V I and Miklaszewski R 1997 *Phys. Rev. E* **56** 1080

[31] Yamazaki R, Taie S, Sugawa S and Takahashi Y 2010 *Phys. Rev. Lett* **105** 050405

[32] Brtka M, Gammal A and Tomio L 2006 *Phys. Lett. A* **359** 339

[33] Gammal A, Tomio L and Frederico T 1999 *Phys. Rev. E* **60** 2421

[34] Muruganandam P and Adhikari S K 2009 *Comput. Phys. Commun.* **180** 1888
Vudragović D, Vidanović I, Balaž A, Muruganandam P and Adhikari S K 2012 *Comput. Phys. Commun.* **183** 2021

[35] Anderson E *et al* 1999 *LAPACK Users' Guide* (Philadelphia, PA: SIAM)

[36] Camassa R and Holm D D 1993 *Phys. Rev. Lett.* **71** 1661

[37] Salerno M 1992 *Phys. Rev. A* **46** 6856

[38] Gomez-Gardeñes J, Malomed B A, Floría L M and Bishop A R 2006 *Phys. Rev. E* **73** 036608

[39] Gammal A, Frederico T, Tomio L and Chomaz P 2000 *Phys. Rev. A* **61** 051602
Gammal A, Frederico T, Tomio L and Chomaz P 2000 *J. Phys. B* **33** 4053–67

[40] Vakhitov N G and Kolokolov A A 1973 *Izv. Vyssh Uchebn. Zaved. Radiofiz.* **16** 1020
Vakhitov N G and Kolokolov A A 1975 *Radiophys. Quantum Electron.* **16** 783